

## HADRON PRODUCTION BY 150 GeV MUONS IN NUCLEAR EMULSION

P.L. JAIN, K. SENGUPTA and G. SINGH

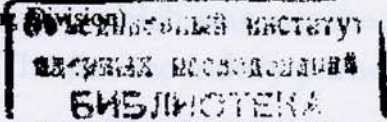
*High Energy Experimental Laboratory, Department of Physics, State University of New York  
at Buffalo, Buffalo, New York 14260, USA*

Received 16 January 1987  
(Revised 8 September 1987)

This paper reports measurements of the hadrons produced in the inelastic scattering of 150 GeV positive muons in nuclear emulsion. Multiplicity distributions of secondary particles are given and are compared with the results of pion and proton interactions in emulsion at different energies. We find similarities as well as differences between muon and hadron collisions with nuclei.

### 1. Introduction

At present there is a great deal of interest in high-energy particle-nucleus interactions. The main interest is due to the fact that the large dimensions of the nuclei allow them to be used as analyzers of the space-time development of interactions. For a hadron, the main production on nuclear targets comes from a mechanism in which a large longitudinal interaction region of the incident particles is involved. However, there exist some other production mechanisms where short interaction regions are available; for example, through intra-nuclear cascading, where the projectile particle interacts with just one nucleon of the target and the products of this interaction (and not the incident particle) interact again with the other nucleons of the target and produce more particles. If we use the hadron as a projectile, then it is difficult to identify the processes of cascading. On the other hand by using muons whose momentum transfers and energy losses are measurable, there is a possibility of identifying cascading by varying the Brojken scaling variable  $\omega$ . With muons, the interaction takes place via the exchange of a single virtual photon with square of mass  $(-q^2)$  and energy  $(E - E' = \nu)$  as continuous variables. Instead of the two Lorentz invariants ( $q^2$  and  $\nu$ ) which define the scattering process, we shall make use of the small dimensionless scaling variable  $\omega = 2M\nu/q^2 = 1/x$  (where  $M$  is the mass of the nucleon) and shall deal with processes in which the virtual photon interacts with only one nucleon of the target nucleus. We thus report here multiparticle production by muons with nuclei at different





values of the Bjorken scaling variable  $\omega$  (hence different distances over which the incident virtual photon is absorbed). In general, we are interested to compare the results of muon-induced and hadron-induced multiparticle production of nuclei.

## 2. Experimental details

A small stack consisting of 24 G-5 emulsion of dimensions  $10 \text{ cm} \times 10 \text{ cm} \times 1.44 \text{ cm}$  was exposed to a 150 GeV positive muon beam at Fermilab. The beam flux density was  $\sim 5 \times 10^5$  muons/cm<sup>2</sup> and was parallel to the emulsion plane. The contamination of the pions in the muon beam was negligible. Each pellicle was area scanned and events with at least one evaporation track were recorded if: (i) a light straight track (muon track) parallel to other primary tracks led into the interaction, (ii) all the secondary tracks and the light primary track came from the same vertex. In order to avoid the background of the secondary events produced by the outgoing muons from the primary interactions, we scanned only the first 5 cm of the plate. Each event was further checked by following the track backward up to the edge of the pellicle. This ensures that the track under consideration is the primary and not a secondary track. Further, all the events were examined under  $100 \times$  oil objective in order to reject the background events having their vertices too far away from the primary muon tracks. The selected events were classified according to the well known nomenclature for black, grey or light tracks: (a) for light tracks,  $g_s \leq 1.5g_0$ , where  $g_s$  is the number of grains per 100 microns of secondary tracks and  $g_0$  is the number of grains per 100 microns of the primary track (the value of  $g_0$  is 20 grains per 100  $\mu$ ); (b) for grey tracks,  $1.5g_0 < g_s \leq 2.5g_0$ , (c) for black tracks  $g_s > 2.5g_0$ .

The visual selection criterion used to collect individual events is only a preliminary one and rigorous tests were applied to reject background events produced either by cosmic rays or by the secondary tracks from other interactions. The selection criteria we used were the following: (i) The primary muon track should not make an angle greater than 3–6 mrad with the direction of the incident beam; (ii) the primary track when traced back to 5 mm, should be flat and straight and have the same dip angle as other incident tracks; (iii) the grain density  $g_0$  of the primary track, measured along a track length of 2 mm, should correspond to the grain density of other primary beams measured at the same depth. In order to eliminate definitely the background events whose vertices were close to a primary muon track, we employed a final test: the points on the incident and the scattered muon tracks were connected by least square fitted lines. If the distance between the generated vertex of the event was less than 0.1  $\mu$  from the incident muon track, the event was retained for analysis. Using these stringent selection criteria, we have thus selected 390 muon-nucleon inelastic interactions at 150 GeV primary energy. All space angles were measured very accurately (with accuracy range  $\theta \sim 0.5$  mrad) by a Koristka scattering microscope, to which was attached a filar micrometer that could read to an accuracy of 0.1  $\mu$ . The flat secondary particles were identified through the



measurements of their  $p\beta$  values and from blob counting. The steeper tracks having dip angles greater than  $30^\circ$  were followed from pellicle to pellicle until they stopped in emulsion. This was done because the available track length was not sufficient to make  $p\beta$  measurements. The track following method together with blob counting gave us independent ways of identification of the secondary particles, and their energies were determined from their ranges.

### 3. Results

Multiplicity of all the observed events has been categorized in terms of heavy ( $N_b$ ) and shower ( $n$ , grey plus light tracks). The identification of the secondary particles and the procedure of their energy determination have been discussed in section 2. Most of the secondary particles were pions and protons and their production mechanism is the well known  $\Delta(1232)$  resonance. The energy of a secondary particle of mass  $m$  and momentum  $p$  was found from its measured value of  $p\beta$  and is given by:

$$E = \left(\frac{1}{2}\right) \left[ |p|\beta + \left\{ (p\beta)^2 + (2m)^2 \right\}^{1/2} \right].$$

We obtained a lower limit on energy  $\nu = E - E'$  by using the energy of all the charged and neutral particles in conjunction with the nuclear evaporation model [1]. By knowing  $\nu$  and  $q^2$ , one could calculate for each event,  $\omega = 2M\nu/q^2$  and also the square of the total center of mass energy  $s = W^2 = M^2 + 2M\nu - q^2$ . In fig. 1,  $\langle q^2 \rangle$  is shown as a function of  $W^2$ . The kinematic range covered in this experiment is  $0.015 < q^2 < 1$  and  $0.5 < W^2 < 24$  and the average value of  $W$  is  $\langle W \rangle \cong 2.3$  GeV. In table 1 is shown the multiplicity of secondary particles ( $n$ ) produced in interactions of 150 GeV muons with emulsion as a function of  $N_b$  which is a

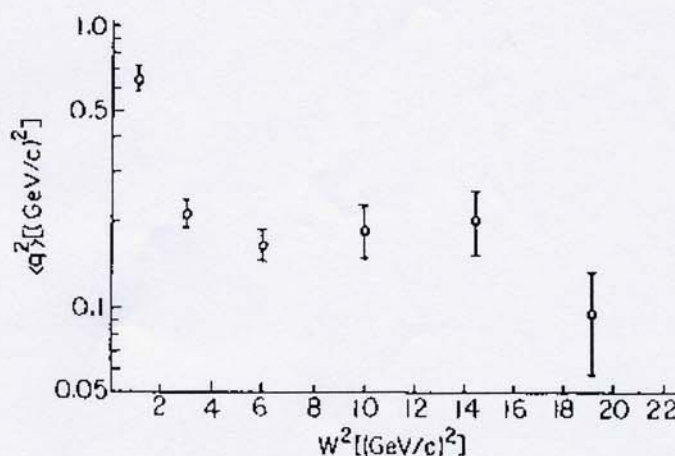


Fig. 1. Plot of invariant mass squared ( $W^2$ ) versus square of four-momentum transfer  $\langle q^2 \rangle$ .



TABLE I

Multiplicity distribution of secondary tracks produced in interactions of 150 GeV muons with emulsion

$n$	$N_b$	0	1	2	3	4	5	6	7	8	9	10	11	12	13	14	15	16	17	18
1	0	0	12	20	25	14	8	4	8	0	1	4	0	0	0	0	0	0	0	0
2	0	3	14	27	22	16	11	7	5	0	1	1	0	0	1	0	0	0	0	0
3	1	3	10	16	7	3	5	9	6	5	2	1	0	2	2	0	0	0	0	0
4	0	0	0	10	5	3	7	3	2	6	0	1	0	0	0	0	0	1	0	0
5	0	1	2	1	3	5	4	3	1	2	2	1	2	1	1	0	2	0	0	0
6	0	0	1	1	2	1	5	2	3	1	1	1	0	0	0	2	0	0	0	0
7	0	0	0	0	1	1	1	1	0	2	0	1	0	0	1	1	1	0	0	0
8	0	0	0	0	0	0	1	0	1	0	2	0	1	0	0	0	1	0	0	0
9	0	0	0	1	0	1	0	0	1	0	0	0	0	0	0	0	0	0	0	0
10	0	0	0	0	0	0	0	0	0	0	0	1	1	0	0	0	0	0	0	0
11	0	0	0	0	0	0	0	1	0	0	0	0	0	0	0	0	0	0	0	0
12	0	0	0	0	0	0	0	0	0	0	0	0	1	0	0	0	0	0	0	0
13	0	0	0	0	0	0	0	0	0	0	0	0	0	0	0	0	0	0	0	0
14	0	0	0	0	0	0	0	0	0	0	0	0	0	0	0	0	0	0	0	0
15	0	0	0	0	0	0	0	0	0	0	0	0	0	1	0	0	0	0	0	1

measure of the excitation of the target nucleus. The average number of secondary charged particles is  $\langle n \rangle = 3.01$ , while the average number of slow particles resulting from the evaporation of the target nucleus is  $\langle N_b \rangle = 5.5$ . Most of the other experiments with high energy muon beam have low efficiency for small number of black tracks. In emulsion, with excellent space resolution we present in fig. 2a the integral distribution of  $N_b$ . This is compared with the hadronic data [2] of primary proton of energy 200 GeV. Both distributions are quite similar within their statistical errors. In fig. 2b is shown the plot of  $\langle n \rangle$  for a given  $N_b$  at different energies: 16.3 GeV pion, 28, 200, 300 GeV proton<sup>2</sup> and 150 GeV muon. The muon data show a linear fit of the form:  $\langle n \rangle = 1.79 + 0.233N_b$ , but the  $N_b$  dependence of muon interactions is obviously weaker than in hadron interactions when both have the same order of primary energy. At higher energies, the slope increases monotonically. The variation of average multiplicity  $\langle n \rangle$  as a function of  $\nu = E - E'$  is shown in fig. 2c for two values of  $\omega$ : (a)  $\omega \leq 5$  and (b) for all  $\omega$  values (where  $\omega$  value is shown in fig. 3a). In both cases  $\langle n \rangle$  increases with  $\nu$  in a similar way. For small  $\omega$ 's, where the virtual photon interacts with only one nucleon, the observed multiplication means that the products of the first collision, on their way out of the nucleus interact with the other nucleons and produce the excess of particles. Within experimental uncertainties, we do not see any difference in the relative multiplication at small and large  $\omega$ 's. This is somewhat interesting, because for large  $\omega$ 's, virtual photons interact diffractively while for small  $\omega$ 's, we deal with incoherent interactions. As data on multiparticle production by muon with proton are not available at all the energies we need, we used for mean charged hadron multiplicity



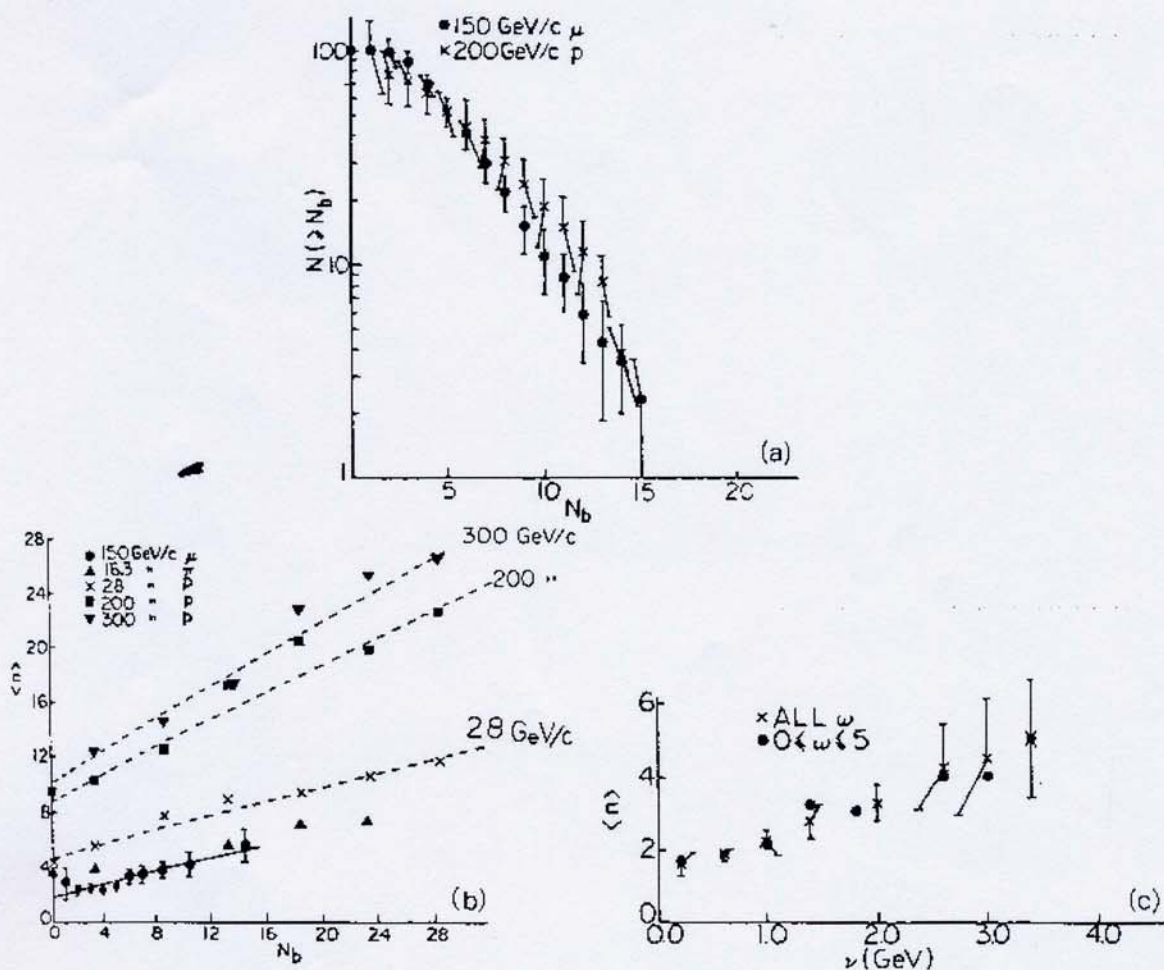


Fig. 2. (a) Integral frequency distribution of  $N_b$ ,  $P(\geq N_b)$  for 200 GeV proton (ref. [7]) and 150 GeV muon beams. The muon data are normalized at  $P_\mu(\geq 5) = P_p(\geq 5)$ . (b)  $\langle n \rangle$  versus  $N_b$  for 16.3 GeV pion, 28, 200 and 300 GeV proton and 150 GeV muon. (c)  $\langle n \rangle$  versus  $\nu = E - E'$  (GeV) for all  $\omega$  and for  $\omega \leq 5$ . The errors have been plotted for the all  $\omega$  data only.

[3-5] the following fitted form:

$$\langle n \rangle = a + b \ln E_{ab} + c (\ln E_{ab})^2, \quad (1)$$

where  $E_{ab} = \sqrt{s} - (m_a + m_b)$  is the c.m.s. energy available for particle production and  $m_a, m_b$  are the masses of the initial particles. The values of constants are taken from ref. [4]:  $a = 0.88$ ,  $b = 0.44$  and  $c = 0.118$ . Eq. (1) gives a good representation of the average charged hadron multiplicity in  $(\mu p)$  interactions [4, 5] in the energy range of  $W$  from 2.5 GeV up to 4.25 GeV.

For more information about the physical nature of the particle multiplication process, we grouped the muon interactions according to the Bjorken scaling variable  $\omega$ . According to ref. [6],  $\omega$  is proportional to the lifetime  $\tau$  of the virtual photon and is equal to  $\omega = m\tau$ .  $\tau$  measures the distance over which the virtual photon can interact coherently with the target nucleons. In fermis this distance is  $r = \frac{1}{3}\omega$ . For

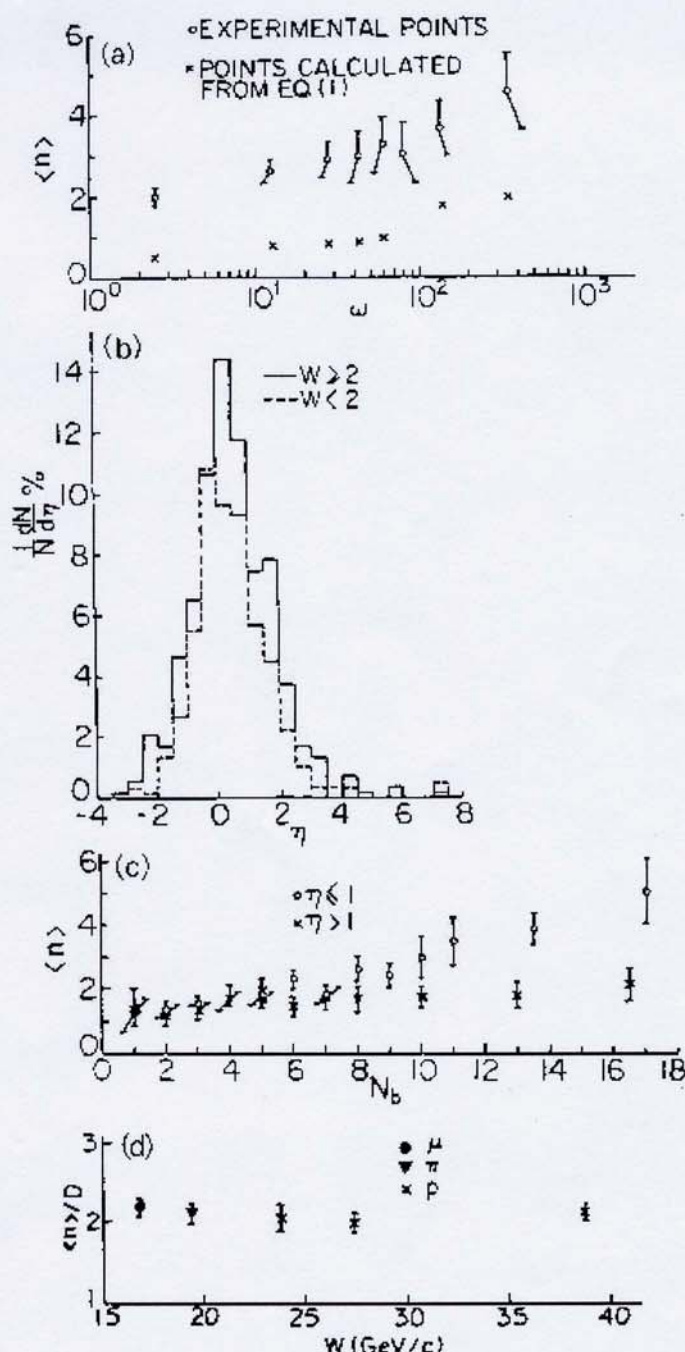


Fig. 3. (a)  $\langle n \rangle$  versus  $\omega$  for (i) 150 GeV muon (experimental data) (ii) The points are calculated from eq. (1). The points ( $\times$ ) are calculated with constants taken from ref. [4]. (b) Pseudorapidity distributions for  $W \geq 2$  and  $W < 2$ . (c)  $\langle n \rangle$  versus  $N_b$  for (i)  $\eta \leq 1$  and (ii)  $\eta > 1$ . (d)  $\langle n \rangle / D$  versus  $W$  for 150 GeV muon, 200 GeV pion, 300, 400 and 800 GeV proton (ref. [8]).

interactions with  $\omega < 5$ , the virtual photon interacts with just one nucleon. In fig. 3a, we show the experimental plot of  $\langle n \rangle$  as a function of  $\omega$ . There is a difference in the relative multiplication between the large and small  $\omega$  values. In this figure, we also show the values of  $\langle n \rangle$  obtained from eq. (1) for the different values of  $W$  in a given  $\omega$  bin. The lowest  $\omega$  bin, therefore, corresponds to interactions of the muon with just one nucleon. In fig. 3a,  $\langle n \rangle$  is always larger than the calculated values of the muon-proton ( $\mu p$ ) collision which means  $\langle R \rangle = [\langle n \rangle_{\mu Em} / \langle n \rangle_{\mu p}] > 1$ , and multiplication of particles takes place for all  $\omega$ 's. The difference between the experimen-



tal data points and the calculated values from eq. (1) is almost constant, indicating a nuclear fragmentation region effect.

In order to compare qualitatively the energy dependence of muon induced pseudorapidity distributions we have divided the events into two energy bins  $W \leq 2$  and  $W > 2$  GeV and plotted their pseudorapidity ( $\eta = -\ln \tan \frac{1}{2}\Theta$ ) distribution in laboratory system as shown in fig. 3b. We observe that the right-hand side of the distribution slightly shifts with an increase of energy, while the left-hand side of the distribution is practically the same and this is just what we find in hadron induced interactions.

In order to study where in the pseudorapidity distribution nuclear effects show up, we follow the well known technique in hadron-emulsion interaction of nuclear effects, using the number of heavily ionizing tracks  $N_b$ . In fig. 3c we plot the distribution of  $\langle n \rangle$  versus  $N_b$  and study the correlation for two different intervals of  $\eta$  i.e.  $\eta < 1.0$  and  $\eta > 1.0$  intervals. For  $\eta \leq 1.0$  (backward hemisphere in the c.m.s.),  $\langle n \rangle$  depends linearly on  $N_b$  and it is due to cascading process in the target nucleus while for  $\eta > 1.0$ ,  $\langle n \rangle$  becomes independent of  $N_b$ . There is a qualitative similarity between lepton and hadron production with nuclei. In fig. 3d, we compare the values of  $\langle n \rangle / D$  versus  $W (= \sqrt{s})$  for muon with hadrons values of  $W$  at 19.4 GeV pion, 23.8, 27.4 and 38.8 GeV<sup>8</sup> proton. Here,  $D = [\langle n^2 \rangle - \langle n \rangle^2]^{1/2}$  is the dispersion of the multiplicity distribution. These values are further comparable with the muon-proton data of ref. [5] at low values of  $W$ . As mentioned above, for all hadronic reactions, this quantity (i.e.  $\langle n \rangle / D$ ) lies between 2 to 2.3 for all  $W$  values.

In conclusion, we can say that there is some similarity between muon and hadron induced multiparticle distributions on nuclei. The average transverse momentum of the muon produced hadrons [9] is the same as that in hadron-hadron data. There is also similarity between the energy dependence of muon and hadron-induced pseudorapidity distributions and thus the production of hadrons by virtual photons is not grossly different from that by hadrons.

We are very grateful to the staff of the Fermilab for the exposure of our emulsion stack. We also thank Dr. G. Das and Dr. M.M. Aggarwal for their partial help at early stages of this experiment. The research work was supported in part by the National Science Foundation under Grant Number NSF/PHY8544391. K.S. would like to thank the Office of Research and Graduate Studies, SUNY at Buffalo for the partial support.

## References

- [1] C.F. Powell, P.H. Fowler and D.H. Perkins, The study of elementary particles by photographic method (Pergamon 1959) p. 464;  
R.M. Brown et al., Phil Mag. 40 (1949) 862
- [2] P.L. Jain et al., Phys. Rev. Lett. 33 (1974) 660;  
P.L. Jain et al., Lett. Nuovo Cim. 12 (1975) 653

- [3] L. Hand et al., *Z. Phys.* C139 (1979) 142; *Acta Phys. Pol.* B9 (1978) 1087
- [4] W. Thormé et al., *Nucl. Phys.* B129, (1977) 365
- [5] C. del Papa et al., *Phys. Rev.* B13 (1976) 2934
- [6] A. Bialas and W. Czyz, *Nucl. Phys.* B137 (1978) 359
- [7] P.L. Jain et al., *Phys. Rev.* D34 (1986) 2886
- [8] P.L. Jain et al., *Phys. Lett.* 187B (1987) 175
- [9] P.L. Jain and K. Sengupta, *Z. Phys.* G36 (1987) 45